Title

Inhomogeneous static magnetic field-induced distortion correction applied to diffusion weighted MRI of the breast at 3T

Journal

Magnetic Resonance in Medicine, 74(4)

ISSN

0740-3194

Authors

Teruel, Jose R
Fjøsne, Hans E
Østlie, Agnes
et al.

Publication Date

2015-10-01

DOI

10.1002/mrm.25489

Peer reviewed

PRECLINICAL AND CLINICAL IMAGING – Note

Magnetic Resonance in Medicine 74:1138–1144 (2015)

Inhomogeneous Static Magnetic Field-Induced Distortion Correction Applied to Diffusion Weighted MRI of the Breast at 3T

Jose R. Teruel,[1,2]* Hans E. Fjøsne,[3,4] Agnes Østlie,[5] Dominic Holland,[6] Anders M. Dale,[1,6,7] Tone F. Bathen,[1] and Pål E. Goa[5,8]

Purpose: To evaluate the performance of an advanced method for correction of inhomogeneous static magnetic field induced distortion in echo-planar imaging (EPI), applied to diffusion-weighted MRI (DWI) of the breast.

Methods: An algorithm for distortion correction based on the symmetry of the distortion induced by static field inhomogeneity when the phase encoding polarity is reversed was evaluated in 36 data sets of patients who received an MRI examination that included DWI ($b = 0$ and 700 s/mm^2) and an extra $b = 0$ s/mm^2 sequence with opposite phase encoding polarity. The decrease of the L_2-square norm after correction between opposed phase encoding $b = 0$ images was calculated. Mattes mutual information between $b = 0$ images and fat-suppressed T_2-weighted images was calculated before and after correction.

Results: The L_2-square norm between different phase encoding polarities for $b = 0$ images was reduced 94.3% on average after distortion correction. Furthermore, Mattes mutual information between $b = 0$ images and fat-suppressed T_2-weighted images increased significantly after correction for all cases ($P < 0.001$).

Conclusion: Geometric distortion correction in DWI of the breast results in higher similarity of DWI to anatomical non-EPI T_2-weighted images and would potentially allow for a more reliable lesion segmentation mapping among different MRI modalities. **Magn Reson Med 74:1138–1144, 2015.** © **2014 Wiley Periodicals, Inc.**

Key words: distortion correction; diffusion-weighted imaging; breast; echo-planar imaging

INTRODUCTION

Diffusion-weighted MRI (DWI) probes the mobility of water molecules in biological tissues, allowing the characterization of tissue structure based on the extent and directionality of microscopic random water diffusion (1). To perform DWI within a time frame that is tolerable for the patient, the majority of studies have adopted echo-planar imaging (EPI) for k-space sampling. The benefits of using EPI are widely known, including reduced imaging time and decreased motion artifacts. However, DWI using EPI is subject to pronounced artifacts due to chemical shift in the phase encoding direction and geometric distortion arising from subject-specific inhomogeneous magnetic susceptibility and gradient field eddy currents (2,3).

DWI is becoming an important imaging modality for breast applications. Several studies have confirmed that apparent diffusion coefficient (ADC) values are lower in malignant lesions compared with benign lesions and healthy fibroglandular tissue due to their increased cellularity (4–8). ADC values have also been reported for prediction and monitoring of breast cancer response to treatment (9–12). More recently, diffusion tensor imaging has been applied for breast tissue characterization and lesion detection (13–15). An additional use of DWI for breast applications employs intravoxel incoherent motion to obtain the contribution from perfusion in diffusion measurements (16,17).

The rapid increase in the use of DWI for breast applications calls for proper management of EPI-related artifacts, because these artifacts will significantly affect the quality and utility of the images. However, correction for spatial and intensity distortion due to inhomogeneous subject magnetization currently is not implemented for breast examinations in clinical routine. This distortion occurs in areas where susceptibility changes are present (e.g., air–tissue boundaries or interfaces between different tissues with different magnetic susceptibilities), producing an artifactual warping of the image.

[1]Department of Circulation and Medical Imaging, Norwegian University of Science and Technology, Trondheim, Norway.

[2]St. Olavs University Hospital, Trondheim, Norway.

[3]Department of Surgery, St. Olavs University Hospital, Trondheim, Norway.

[4]Department of Cancer Research and Molecular Medicine, Norwegian University of Science and Technology, Trondheim, Norway.

[5]Clinic of Radiology and Nuclear Medicine, St. Olavs University Hospital, Trondheim, Norway.

[6]Department of Neurosciences, University of California, San Diego, La Jolla, California, USA.

[7]Department of Radiology, University of California, San Diego, La Jolla, California, USA.

[8]Department of Physics, Norwegian University of Science and Technology, Trondheim, Norway.

Grant sponsors: Central Norway Regional Health Authority and the Liaison Committee between the RHA and the Norwegian University of Science and Technology.

*Correspondence to: Jose R. Teruel, Department of Circulation and Medical Imaging, Faculty of Medicine, Norwegian University of Science and Technology, Post Box 8905, MTFS, 7491 Trondheim, Norway. E-mail: jose.teruel@ntnu.no

Received 16 June 2014; revised 26 August 2014; accepted 17 September 2014

DOI 10.1002/mrm.25489

Published online 16 October 2014 in Wiley Online Library (wileyonlinelibrary.com).

Distortion correction in EPI has been explored widely since the first and most known approach described by Jezzard and Balaban (18), and advanced methods have shown high accuracy to correct geometric distortion in EPI of the brain (19,20). The aim of this study was to evaluate the performance of an advanced method for correction of inhomogeneous static magnetic field-induced distortion in DWI of the breast, using images acquired with opposite phase encoding polarities.

METHODS

Patient Cohort

As part of an ongoing study in our institution, 37 patients with a known lesion in at least one breast underwent an MR examination including DWI using EPI. Patients for this study were included regardless to lesion characteristics, breast density, or any other clinical factor.

All participating subjects provided signed informed consent, and the study was approved by the Regional Committee for Medical and Health Research Ethics, Central Norway, reference number 2011/568.

Image Acquisition

All patients were imaged on a 3T scanner (Siemens Skyra, Erlangen, Germany) equipped with a dedicated 16-channel bilateral breast coil. The imaging protocol collected fat-suppressed unilateral sagittal images using a twice-refocused spin echo sequence with EPI (repetition time/echo time = 9300/85 ms; matrix: 90 × 90; in-plane res: 2 × 2 mm; slice thickness: 2.5mm; 60 slices; NEX = 1; Spectral fat saturation; GRAPPA parallel imaging acceleration factor 2 with autocalibration using 24 phase encoding reference lines) including two or three b-values (b = 0, 200[for n = 26 cases], and 700 s/mm^2), with Anterior-Posterior (AP) phase encoding polarity, and 30 unique diffusion directions for each non-zero b-value. Total acquisition time for this sequence was 5:35 minutes (10 min when including b = 200). Immediately after this acquisition an extra image with b = 0 s/mm^2 was acquired with the same parameters, but reverse phase encoding polarity i.e., Posterior-Anterior (PA) for implementation of distortion correction. The scan time for this extra acquisition was 56 seconds. The b = 0 image with AP encoding direction will be referred as 'b_0 forward' image, while the b = 0 image acquired with PA encoding polarity will be referred as 'b_0 reverse' image from now on.

Unilateral sagittal two-dimensional T_2-weighted turbo spin-echo images, with and without fat suppression, were acquired with the same slice thickness and field of view to allow for a perfect matching slice-by-slice with the diffusion images (in-plane resolution = 0.7 × 0.7 mm).

T1-weighted dynamic contrast-enhanced MRI (DCE-MRI), with the same slice thickness and field of view as the DWI and T_2-weighted images, was acquired with a 3D radiofrequency spoiled gradient-echo sequence without fat suppression (flip angle = 15°; repetition time/echo time = 5.82/2.18 ms; in-plane resolution = 0.7 × 0.7 mm). After the acquisition of one baseline image, a bolus injection of 0.1 mmol/kg body weight gadolinium-based contrast agent Dotarem (Guerbert LLC, Bloomington, Indiana, USA) was given automatically at a rate of 2 mL/s followed by a 20 mL saline flush. At the time of injection, the acquisition of seven post-contrast images started with a temporal resolution of 1 min.

Distortion Correction

The algorithm for distortion correction implemented in this study was described and evaluated in brain EPI images by Holland et al. (20). The method makes use of the symmetry of the distortion induced by static field inhomogeneity when the phase encoding polarity is reversed; the deformation field is calculated iteratively for different Gaussian smoothing kernels applied to the pair of opposing phase encoding b_0 images (reducing the standard deviation of the kernel and updating the distortion field at each step). Subsequently, the calculated deformation field is applied to correct the entire set of diffusion images. The distortion correction was performed using the preprocessing algorithm provided in the Computational Morphometry Toolkit (CMTK; SRI International, Menlo Park, California, USA) available at http://nitrc.org/projects/cmtk/.

Quantitative Analysis

For each patient, a single sagittal image slice was selected. The slice was selected proximal to the middle part of the breast (nipple/areolar region) to maximize the amount of anatomy presented within the field of view. To evaluate the performance of the proposed solution for distortion correction, two similarity metrics were calculated for each subject using MATLAB (MathWorks, Natick, Massachusetts, USA).

The L_2-square norm between both b_0 images (forward and reverse) was calculated before and after distortion correction as

$$L_2^2 = \sum\nolimits_{ij} \left(F_{ij} - R_{ij}\right)^2, \quad [1]$$

where F_{ij} represents the value of the (i,j)th voxel of the b_0 forward image and R_{ij} represents the value of the (i,j)th voxel of the b_0 reverse image. The percentage change of the L_2-square norm after correction was calculated as

$$100(L_2^2 u - L_2^2 c)/L_2^2 u, \quad [2]$$

where $L_2^2 u$ is the L_2-square norm between the original b_0 forward and reverse images and $L_2^2 c$ is the L_2-square norm between the corrected b_0 forward and reverse images.

To determine whether the b_0 image represents the true anatomy with an improved fidelity after distortion correction, the similarity of the b_0 forward image before and after correction with respect to the fat-suppressed T_2-weighted image was determined using the Mattes mutual information (MMI) similarity metric (21). First, the T_2-weighted image was resampled using bicubic interpolation to match the in-plane resolution of the b_0 diffusion image. Second, a two-dimensional rigid registration of the b_0 image to the T_2-weighted image was performed by employing the MMI similarity metric for both the original and corrected b_0 images. The MMI metric values after the registration in both situations (i.e., with

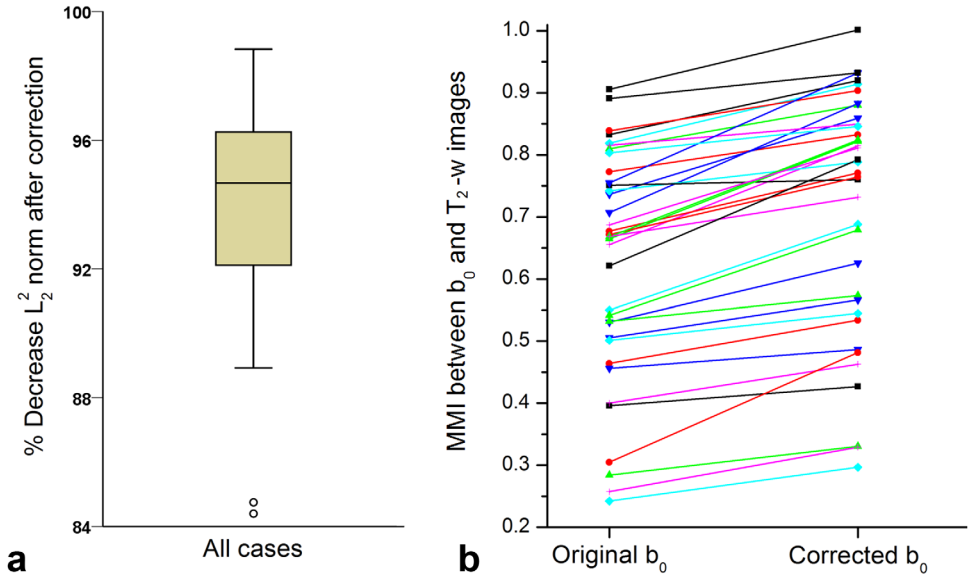

FIG. 1. **a:** Percentage decrease of the L_2-square norm between both b_0 images (forward and reverse) after applying distortion correction for every case. **b:** Mattes mutual information similarity metric between the b_0 forward image and the corresponding fat-suppressed T_2-weighted image when using both the original b_0 forward image and the corrected b_0 forward image.

and without applying distortion correction) were compared by the Wilcoxon signed ranks test using SPSS version 20 (IBM, Chicago, Illinois, USA).

RESULTS

Analysis was performed for 36 patients, as severe motion in one case was reported and did not allow for reliable distortion correction between the misaligned b_0 forward and reverse images.

The L_2-square norm between both b_0 diffusion images acquired with opposite phase encoding polarities was significantly reduced after distortion correction, with a mean decrease of $94.3 \pm 2.4\%$ (Fig. 1a). In Figure 2, an example of the overlap of both b_0 diffusion images before and after applying the distortion correction is shown. The right column in Figure 2 shows the overlap between the original b_0 images with opposed polarity, and after correction. In this representation, matching intensities would produce a grayscale tone, whereas unmatched

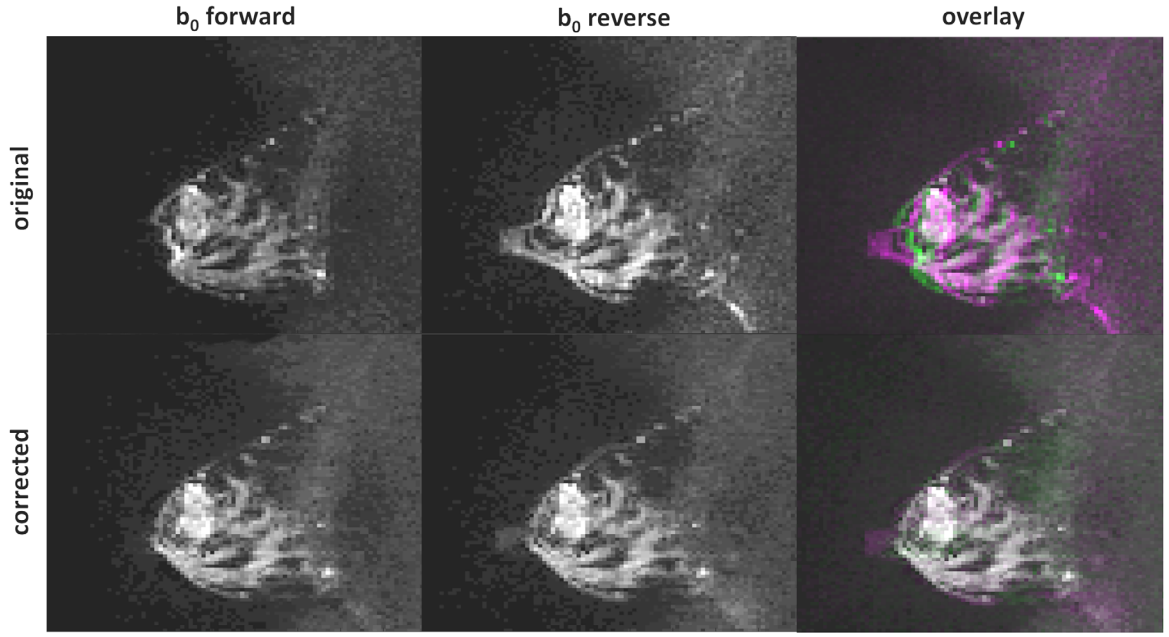

FIG. 2. Visual comparison between the b_0 forward and reverse images before and after correction. Overlay images present a grayscale value for closely matched signal intensities and a color value (green for b_0 forward and purple for b_0 reversal) for dissimilar signal intensities. The percentage decrease of the L_2-square norm obtained after correction for this case was 94.6%.

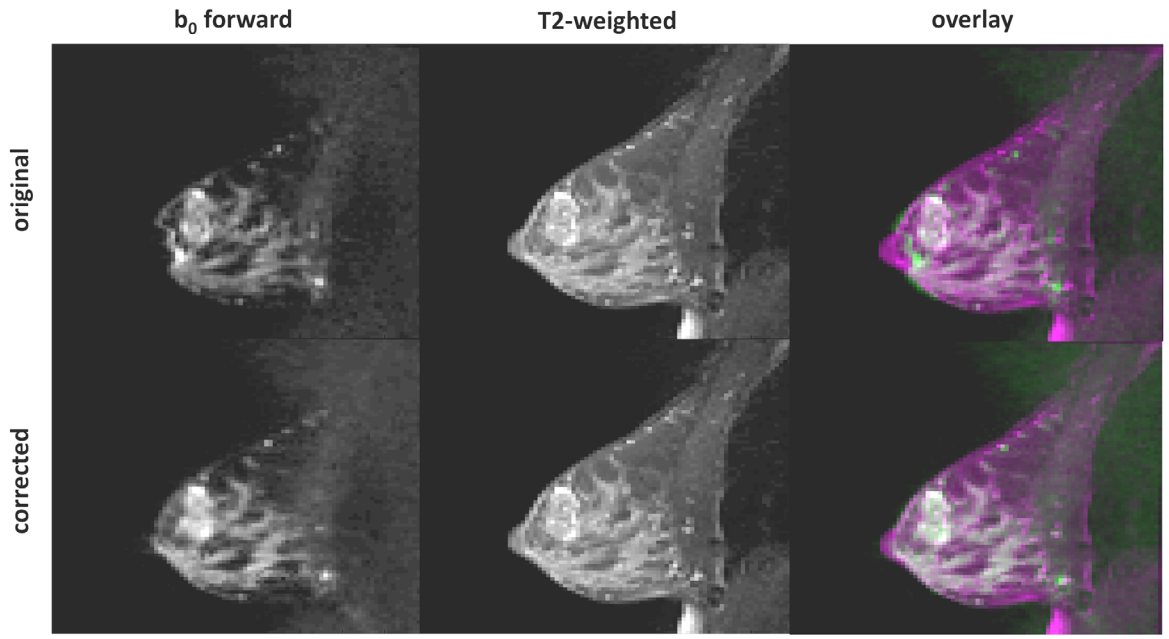

FIG. 3. Visual comparison between the b_0 forward image and the fat-suppressed T_2-weighted image before and after correction. Color overlay interpretation follows the same pattern explained for Figure 1. Mattes mutual information between b_0 forward and T_2-weighted images was increased to 0.81 after correction from an original value of 0.66.

overlay would produce a color intensity value (green for the AP direction and purple for the PA direction). The almost complete absence of color in the bottom right image in Figure 2 demonstrates a practically perfect matching after correction.

The similarity between the fat-suppressed T_2-weighted images and the b_0 images measured by the MMI metric was, for all cases, higher after correction (Fig. 1b), indicating that b_0 images were always more similar to their corresponding T_2-weighted images after applying distortion correction. Furthermore, a statistically highly significant difference ($P < 0.001$) was found when comparing MMI pairwise (MMI of the original and corrected b_0 with respect to T_2 weighting). Figure 3 presents an overlay of the b_0 forward images, before and after correction, on the corresponding T_2-weighted image for one case.

To show the importance of distortion correction in order to obtain reliable direct mapping from different MRI modalities such as DCE-MRI to DWI, a selected case presenting a malignant lesion clearly visible in the b_0 image due to surrounding suppressed fatty tissue is shown in Figure 4. This figure shows how the lesion was manually segmented using DCE-MRI (after resampling and rigid registration, using MMI, to DWI), how it was manually segmented directly in the b_0 diffusion images, and the overlay of both segmentations over the b_0 diffusion images. Our analysis revealed how the lesion was compressed due to distortion in the b_0 original image, where the total area covered by the segmentation was 0.84 cm^2, whereas it was 1.20 cm^2 for the DCE-MRI and 1.12 cm^2 for the b_0 corrected image. Furthermore, when the ROI of the lesion obtained from DCE-MRI was mapped on the b_0 images, the deviation observed with regard to the ROI directly obtained using the b_0 images was higher in the original b_0 image, while for the b_0 corrected image, the DCE-MRI mapped ROI over the b_0 image was similar to the direct segmentation (Figure 4).

DISCUSSION

Our results show how geometric distortion affects DWI of the breast when using EPI for k-space filling. This is clearly illustrated in the top row of Figure 2, where the nipple appears completely wrapped into the breast when applying AP polarity for the phase encoding gradient (b_0 forward), and conversely it is stretched far outside its real location when using a PA phase encoding polarity (b_0 reverse). Without distortion-induced artifacts, both images should theoretically be identical. In the breast, the nipple area is the most obvious region to observe this effect visually due to its high deformation and known anatomy. However, the mismatch observed in the right top panel in Figure 2 suggests that the distortion affected the majority of the image.

After applying distortion correction (Fig. 2) both b_0 images became practically identical. For all of the cases under study, a mean decrease of the L_2-square metric of 94.3% (where 100% means that the images would have become exactly the same) was obtained (Fig. 1a). Nevertheless, that both b_0 images became practically identical for all cases does not directly imply that the corrected images better represent the true anatomy. To evaluate this, the similarity between the b_0 forward image, before and after correction, and the fat-suppressed T_2-weighted image was quantified using a mutual information metric described by Mattes et al. (21). The results presented in Figure 1b show how the similarity between the T_2-weighted anatomical

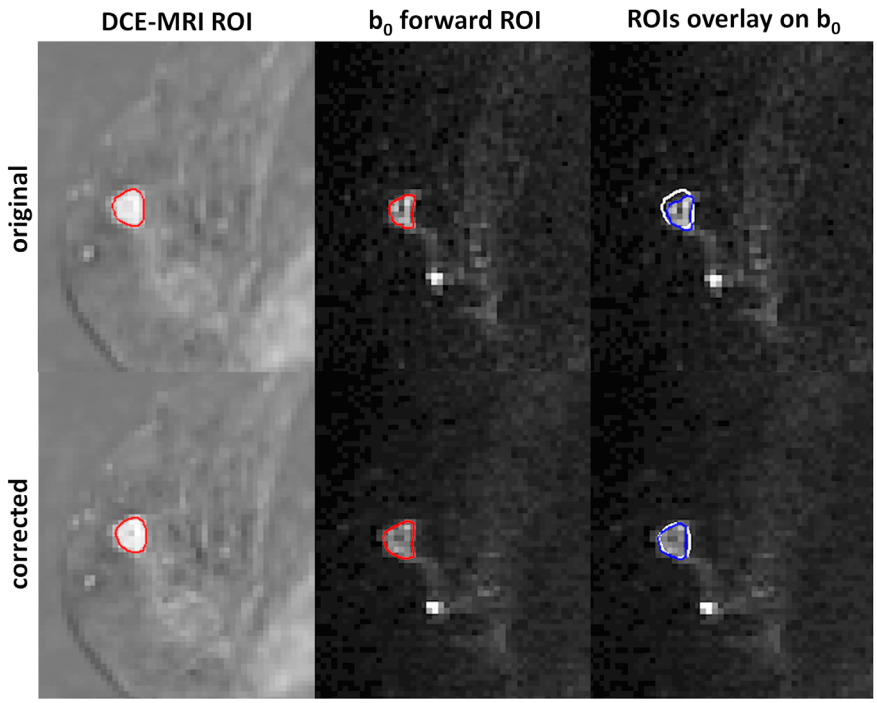

FIG. 4. Tumor delineation for a specific case. The top row presents the segmentation obtained directly over the 2-min DCE-MRI post-contrast subtracted image (left), the segmentation obtained directly over the original b_0 forward image (center), and the mapping of both segmentations (DCE-MRI segmentation in white, original b_0 segmentation in blue) overlaid on the original b_0 image (right). The bottom row shows the same workflow when using the distortion corrected b_0 image.

image and the b_0 forward image was significantly increased for all cases after distortion correction, demonstrating that the corrected diffusion images represent the true anatomy more reliably. In Figure 3, a particular case is shown to demonstrate how distortion correction leads to an image that better represents the true anatomy. Our analysis focused on areas clearly affected by distortion, i.e., slices with large anatomy including the nipple or lesions. In

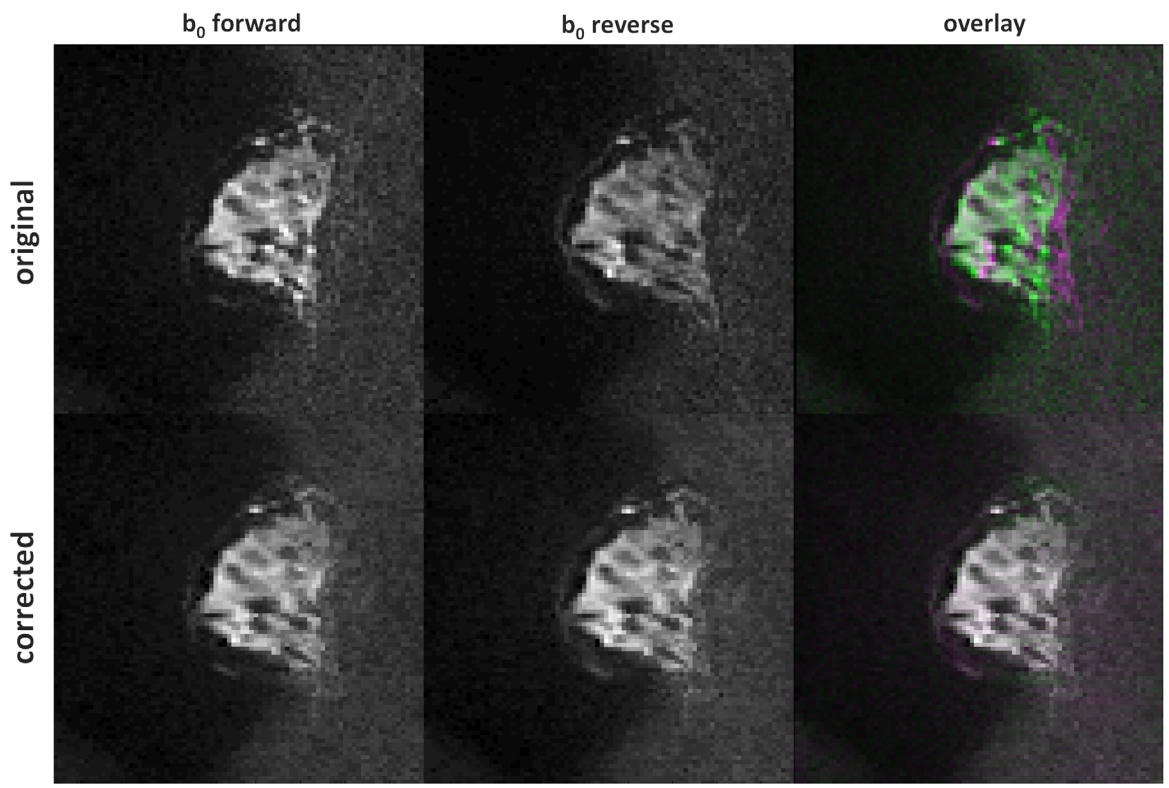

FIG. 5. Example case of the performance of the distortion correction method in a slice apart from the nipple or any pathology. The percentage decrease of the L_2-square norm obtained after correction for this case was 94.5%.

Figure 5, we have included one case of a lateral slice far from the nipple or any pathology to illustrate that the results hold for different areas. The performance of the distortion correction algorithm for different cases is shown in Supporting Figures S1–S4.

DWI is widely used for several applications in breast imaging. The effect of geometric distortion would produce mainly two problems with regard to lesion evaluation. First, there would be an artifactually higher partial volume effect, as different regions could be partially overlapped: one voxel not affected by distortion would be correctly localized, while one voxel close to an interface between tissues could be misaligned (completely or partially) and contribute to the signal of a different voxel. In this manner, as shown in Figure 4, lesions may appear compressed due to geometric distortion. In the same way, a lesion could also appear expanded, leading to a loss of signal and to a larger region with increased partial volume effects. Second, EPI-induced distortion in diffusion images would not allow for a highly accurate mapping of ROIs obtained from other modalities, as DCE-MRI directly on DWI, as shown in Figure 4.

The aim of this study was to evaluate whether distortion correction would improve image quality of DWI, and how this could influence lesion detection and registration between different series. We demonstrated that inhomogeneous susceptibility-induced geometric distortion affects DWI of the breast. Nevertheless, because most previous breast studies using DWI employ the median ADC value of the segmented lesions, and ROIs are placed directly in diffusion images or derived parametric maps, the fact that some voxels present an artifactually higher partial volume effect or a slight compression of the lesion is not expected to affect analysis using the median ADC value. This statement is in agreement with the findings presented by Arlinghaus et al. (22), where it was reported that an affine image registration for motion and eddy current–induced distortion correction, even though improving the alignment of individual DWIs of the breast, did not noticeably affect the median ADC value of the lesions. Further studies are warranted to evaluate how different DWI-derived parameters are affected when applying distortion correction.

To the best of our knowledge, correction for inhomogeneous static field induced geometric distortion has not been implemented or evaluated in breast DWI using EPI. The main contribution of our study relies on the potential of improvement of three known challenges when analyzing diffusion images. First, accurate diffusion analysis is complicated for very small lesions. Low resolution of DWI imposes a limitation for detection of lesions directly in DWI. Distortion correction could provide a benefit for these cases, as it would reduce artifactual partial volume effects and lesion compression. Second, if a lesion is artificially expanded due to distortion, this would lead to a loss of signal voxel by voxel. Low signal-to-noise ratio is already known to be a generic limitation of DWI, and too low signal intensity would limit reliable exponential fitting (for a high b value closer to the noise floor when losing signal). Finally, for lesions not visible directly in diffusion images, distortion correction would allow for a more reliable ROI mapping, as well as more reliable voxel by voxel comparison between different MRI modalities.

When implementing EPI in a DWI sequence, the eddy current originating from the different diffusion gradients induces an additional geometric distortion that is dependent on the direction and strength of the applied diffusion gradient. Our DWI sequence employs a twice-refocused spin echo technique to reduce the eddy current–induced distortion (23). In this way, the computed correction for the b_0 images can subsequently be applied to the rest of the diffusion images independently of their diffusion weight and diffusion gradient direction. If a twice-refocused spin echo is not used, it would still be possible to use the distortion correction method in combination with eddy current correction (24).

Limitations of the application of the distortion correction method to breast studies include the variable breast morphology, as well as the algorithm parameters selection. Even though the method proved to be successful for all cases, there is variability in the performance for different cases. We presume that this variability may be due to the variable anatomy of the breast (dense/fatty, small/big). In addition, the algorithm (see CMTK epiunwarp documentation for a description of the input parameters) were kept fixed for all cases, while better individual performance might be attained if tuning them separately for each case. Regarding the protocol setup and implementation, it is important to note that we acquired both b_0 images as the first and last image of the DWI acquisition, making them more susceptible to patient motion. However, the fixed placement and padding of the breasts, as well as the tolerable scanning time, did not lead to severe motion of the patient, and only one patient had to be excluded for this reason. In any case, the acquisition can also be implemented to acquire both b_0 images consecutively to reduce the possibility of patient motion corrupting the distortion-correction field. Finally, our study was implemented using a unilateral sagittal acquisition due to the requirements imposed by different lines of investigation at our institution. Nevertheless, the application of distortion correction is independent of in-plane orientation being directly applicable to the most common bilateral axial orientation.

CONCLUSION

We have demonstrated that breast DWI would benefit from the use of advanced distortion correction methods such as the one we have explored in our study (20). To apply this processing method successfully, only a small additional acquisition time is required, without any necessary adaptations or technical implementations on the scanner, so it easily can be implemented in any protocol.

REFERENCES

1. Le Bihan D, Breton E. Imagerie de diffusion in vivo par resonance magnetique nucleaire. C R Acad Sci (Paris) 1985;301:1109–1112.
2. Le Bihan D, Poupon C, Amadon A, Lethimonnier F. Artifacts and pitfalls in diffusion MRI. J Magn Reson Imaging 2006;24:478–488.
3. Poustchi-Amin M, Mirowitz SA, Brown JJ, McKinstry RC, Li T. Principles and applications of echo-planar imaging: a review for the general radiologist. Radiographics 2001;21:767–779.

4. Guo Y, Cai YQ, Cai ZL, Gao YG, An NY, Ma L, Mahankali S, Gao JH. Differentiation of clinically benign and malignant breast lesions using diffusion-weighted imaging. J Magn Reson Imaging 2002;16:172–178.
5. Woodhams R, Matsunaga K, Kan S, Hata H, Ozaki M, Iwabuchi K, Kuranami M, Watanabe M, Hayakawa K. ADC mapping of benign and malignant breast tumors. Magn Reson Med Sci 2005;4:35–42.
6. Rubesova E, Grell AS, De Maertelaer V, Metens T, Chao SL, Lemort M. Quantitative diffusion imaging in breast cancer: a clinical prospective study. J Magn Reson Imaging 2006;24:319–324.
7. Marini C, Iacconi C, Giannelli M, Cilotti A, Moretti M, Bartolozzi C. Quantitative diffusion-weighted MR imaging in the differential diagnosis of breast lesion. Eur Radiol 2007;17:2646–2655.
8. Partridge SC, Demartini WB, Kurland BF, Eby PR, White SW, Lehman CD. Differential diagnosis of mammographically and clinically occult breast lesions on diffusion-weighted MRI. J Magn Reson Imaging 2010;31:562–570.
9. Pickles MD, Gibbs P, Lowry M, Turnbull LW. Diffusion changes precede size reduction in neoadjuvant treatment of breast cancer. Magn Reson Imaging 2006;24:843–847.
10. Park SH, Moon WK, Cho N, Song IC, Chang JM, Park IA, Han W, Noh DY. Diffusion-weighted MR imaging: pretreatment prediction of response to neoadjuvant chemotherapy in patients with breast cancer. Radiology 2010;257:56–63.
11. Iacconi C, Giannelli M, Marini C, Cilotti A, Moretti M, Viacava P, Picano E, Michelotti A, Caramella D. The role of mean diffusivity (MD) as a predictive index of the response to chemotherapy in locally advanced breast cancer: a preliminary study. Eur Radiol 2010;20: 303–308.
12. McLaughlin RL, Newitt DC, Wilmes LJ, Jones EF, Wisner DJ, Kornak J, Proctor E, Joe BN, Hylton NM. High resolution in vivo characterization of apparent diffusion coefficient at the tumor–stromal boundary of breast carcinomas: a pilot study to assess treatment response using proximity-dependent diffusion-weighted imaging. J Magn Reson Imaging 2013;39:1308–1313.
13. Partridge SC, Ziadloo A, Murthy R, White SW, Peacock S, Eby PR, DeMartini WB, Lehman CD. Diffusion tensor MRI: preliminary anisotropy measures and mapping of breast tumors. J Magn Reson Imaging 2010;31:339–347.
14. Dietzel M, Grässel D, Gajda M, Camara O, Kaiser WA. Diffusion tensor magnetic resonance imaging of the breast: a pilot study. Eur Radiol 2011;21:1–10.
15. Eyal E, Shapiro-Feinberg M, Furman-Haran E, Grobgeld D, Golan T, Itzchak Y, Catane R, Papa M, Degani H. Parametric diffusion tensor imaging of the breast. Invest Radiol 2012;47:284–291.
16. Sigmund EE, Cho GY, Kim S, Finn M, Moccaldi M, Jensen JH, Sodickson DK, Goldberg JD, Formenti S, Moy L. Intravoxel incoherent motion imaging of tumor microenvironment in locally advanced breast cancer. Magn Reson Med 2011;65:1437–1447.
17. Bokacheva L, Kaplan JB, Giri DD, Patil S, Gnanasigamani M, Nyman CG, Deasy JO, Morris EA, Thakur SB. Intravoxel incoherent motion diffusion-weighted MRI at 3.0 T differentiates malignant breast lesions from benign lesions and breast parenchyma. J Magn Reson Imaging 2014;40:813–823.
18. Jezzard P, Balaban RS. Correction for geometric distortion in echo planar images from B0 field variations. Magn Reson Med 1995;34:65–73.
19. Andersson JL, Skare S, Ashburner J. How to correct susceptibility distortions in spin-echo echo-planar images: application to diffusion tensor imaging. NeuroImage 2003;20:870–888.
20. Holland D, Kuperman JM, Dale AM. Efficient correction of inhomogeneous static magnetic field-induced distortion in echo planar imaging. NeuroImage 2010;50:175–183.
21. Mattes D, Haynor DR, Veselle H, Lewellen TK, Eubank W. PET/CT Image registration in the chest using free-form deformations. IEEE Trans Med Imaging 2003;22:120–128.
22. Arlinghaus LR, Welch EB, Chakravarthy AB, et al. Motion correction in diffusion-weighted MRI of the breast at 3T. J Magn Reson Imaging 2011;33:1063–1070.
23. Reese TG, Heid O, Weisskoff RM, Wedeen VJ. Reduction of eddy-current-induced distrotion in diffusion MRI using a twice-refocused spin echo. Magn Reson Med 2003;49:177–182.
24. White NS, McDonald CR, Farid N, Kuperman JM, Kesari S, Dale AM. Improved conspicuity and delineation of high-grade primary and metastatic brain tumors using "restriction spectrum imaging": quantitative comparision with high B-value DWI and ADC. AJNR Am J Neuroradiol 34:958–964.

SUPPORTING INFORMATION

Additional Supporting Information may be found in the online version of this article.

Supporting Figure S1. Example case of the performance of the distortion correction method in a slice presenting only a lesion (fatty breast case). The percentage decrease of the L_2-square norm obtained after correction for this case was 96.6%.

Supporting Figure S2. Example case of the performance of the distortion correction method in a slice presenting only healthy tissue (dense breast case). The percentage decrease of the L_2-square norm obtained after correction for this case was 82.5%.

Supporting Figure S3. Example case of the performance of the distortion correction method in a slice placed within the nipple region and including healthy tissue and a lesion. The percentage decrease of the L_2-square norm obtained after correction for this case was 95.6%.

Supporting Figure S4. Example case of the performance of the distortion correction method in a slice presenting only healthy tissue (fatty breast case). The percentage decrease of the L_2-square norm obtained after correction for this case was 90.1%.